Facile synthesis of ultrasmall polydopamine-polyethylene glycol nanoparticles for cellular delivery

Sean Harvey, David Yuen Wah Ng, Jolanta Szelwicka, Lisa Hueske, Lothar Veith, Marco Raabe, Ingo Lieberwirth, George Fytas, Katrin Wunderlich, and Tanja Weil

Citation: Biointerphases **13**, 06D407 (2018); doi: 10.1116/1.5042640
View online: https://doi.org/10.1116/1.5042640
View Table of Contents: https://avs.scitation.org/toc/bip/13/6
Published by the American Vacuum Society

Facile synthesis of ultrasmall polydopamine-polyethylene glycol nanoparticles for cellular delivery

Sean Harvey,[1] David Yuen Wah Ng,[1] Jolanta Szelwicka,[1] Lisa Hueske,[1] Lothar Veith,[1] Marco Raabe,[1] Ingo Lieberwirth,[1] George Fytas,[1,2] Katrin Wunderlich,[1,a)] and Tanja Weil[1,a)]
[1]*Max Planck Institute for Polymer Research, Ackermannweg 10, 55128 Mainz, Germany*
[2]*IESL-FORTH, 70013 Heraklion, Greece*

(Received 3 June 2018; accepted 3 October 2018; published 25 October 2018)

Very small polydopamine (PDA) polyethylene glycol (PEG) crosslinked copolymer (PDA-PEG) nanoparticles have been prepared following a convenient one-step procedure in aqueous solution. Particle sizes and colloidal stabilities have been optimized by varying PEG in view of chain length and end group functionalities. In particular, amine-terminated PEG3000 [$PEG_{3000}(NH_2)_2$] reacted with polydopamine intermediates so that very small, crosslinked PDA-PEG nanoparticles with sizes of less than 50 nm were formed. These nanoparticles remained stable in buffer solution and no sedimentation occurred. Chemical functionalization was straight-forward as demonstrated by the attachment of fluorescent dyes. The PDA-PEG nanoparticles revealed efficient cellular uptake via endocytosis and high cytocompatibility, thus rendering them attractive candidates for cell imaging or for drug delivery applications. https://doi.org/10.1116/1.5042640

I. INTRODUCTION

Polymeric nanoparticles provide a broad range of applications in the biomedical field as they generally provide a synthetic platform offering high capacity for chemical modifications as well as control over their relative sizes.[1] Based on their ease of synthesis and the opportunities to impart multiple functionalities toward biological targets of interest, polymeric nanoparticles have emerged as versatile tools for cellular imaging[2,3] as well as for delivery applications.[4,5] However, to further increase their acceptance for biomedical usage, the design and synthesis of new materials providing control over very small particle sizes that reveal high tissue penetration, while maintaining biocompatibility and high colloidal stability, are highly favorable. Furthermore, synthesis procedures based on "green" preparation methods without reactive, potentially toxic reagents and organic solvents are essential to eliminate possible carrier-based toxicity. It is therefore intuitive to combine a mild polymerization technique with monomers, either derived from Nature or with proven biocompatibility, to fabricate a category of materials that encompasses the above-mentioned properties.

The incorporation of biopolymers such as polypeptides, DNA, or carbohydrates into the synthesis of polymeric nanocarriers have seen a rapid development, especially as cancer therapeutics.[6,7] Unlike the aforementioned biomacromolecules, natural monomers such as dopamine and melanins that are capable of initiating polymerization processes have received increasing attention only since the past decade.[8] As the polymerization of dopamine into polydopamine (PDA) occurs in very mild aqueous conditions, its potential in nanomedicine was explored intensely as drug delivery,[9] photothermal,[10] cell-growth stimulating,[11] or diagnostic agents[12] due to its biocompatibility and capacity to introduce various functionalities. While the reactivity and the associated chemical groups available on PDA found general consensus among the scientific community, the control of PDA sizes and its notorious aggregation propensity remains highly challenging. Limited attempts have been made by optimizing polymerization conditions using different *p*H and/or additives with final PDA nanoparticles above 100 nm.[13–20] These large PDA nanoparticles facilitated the loading of various aromatic anti-cancer drugs[21] and attractive photothermal properties but are inherently limited by biodistribution mechanisms in the body. On the other hand, PDA nanoparticles with a size of less than 50 nm have been prepared following a process similar to the silicalike reverse microemulsion[22] from cyclohexane water mixtures or with proteins as template.[23–25] Due to the sticky surface of PDA nanoparticles providing many reactive catechol and quinone groups, a second surface functionalization step is usually required to stabilize the particles and to render them inert in complex media. In this way, core-shell nanoparticles with PDA in the core and a poly(ethylene glycol) (PEG) shell have been fabricated.[26] In recent years, more complex structures have been achieved, e.g., poly(lactic-*co*-glycolic acid) core coated with PDA and functionalized with PEG.[27] Besides the core-shell nanoparticles, also PEG nanoparticles[28,29] have been reported by functionalization of the PEG chains with acetyl, acryl, or fluorene groups. In addition, stable core-crosslinked micellar structures using dopamine as a crosslinker were investigated.[30,31] For core-crosslinked micelles, it is reported that small amounts (5% or less) of dopamine are sufficient to stabilize the micelles.[30] Despite these synthetic achievements, the reported methodologies typically involve

a)Electronic addresses: wunderlich@mpip-mainz.mpg.de and weil@mpip-mainz.mpg.de

multistep synthesis with high structural complexity where one or more conditions are not biocompatible.

Herein, very small and narrowly dispersed PDA-PEG nanoparticles with dimensions of about 40 nm were prepared in a single reaction step in aqueous solution without the necessity to add surfactants or organic solvents. The reaction proceeds smoothly providing colloidally stable, crosslinked copolymer nanoparticles. PEG reduces sedimentation and contributes to improved nanoparticle stability[32] in aqueous solution, whereas PDA serves as crosslinker also offering the required functionalities for crosslinking and postfunctionalization. To demonstrate the availability of functionalities, the PDA-PEG nanoparticles were functionalized covalently with a dye, which also enabled studying cellular uptake. High cellular uptake via energy dependent endocytosis processes and low cellular toxicity were observed revealing promising features for cellular imaging and drug delivery applications.

II. EXPERIMENT

A. Materials

α,ω-Bis-amino PEG polymers of MW 2000, 3000, 6000, and 10 000 (Rapp Polymere), α-Methoxy-ω-amino PEG of MW 2000 (Rapp Polymere) and amine-terminated poly(*N*-isopropylacrylamide) (Sigma-Aldrich) have been used as polymers. In addition, the following reagents have been used: dopamine hydrochloride (Alfa Aesar), sodium phosphate monohydrate 98% (Roth), dihydroxybenzene (Sigma-Aldrich), Dihydroxybenzylamine hydrobromide (Sigma-Aldrich), dihydroxy-L-phenylalanine (Sigma-Aldrich), Tris (hydroxymethyl)aminomethane (TRIS) (ICN Biomedicals), ninhydrin (Alfa Aesar), doxorubicin hydrochloride (≥99.0%, XingCheng ChemPhar Co. Ltd., Taizhou, China), acetic anhydride (VWR), succinic anhydride (Sigma-Aldrich), ethyl acetate (VWR), Horseradish Peroxidase Type II (Sigma-Aldrich), human serum albumin (Sigma-Aldrich), fluorescein isothiocyanate (Sigma-Aldrich), rhodamine isothiocyanate (Sigma-Aldrich), Dulbecco's Modified Eagle's Medium (DMEM) cell culture media (Life Technologies), fetal bovine serum (FBS) (Gibco®), penicillin/streptomycin solution (100×) was purchased from PAA Laboratories GmbH (Cölbe, Germany), Eagle's minimum essential medium [non-essential amino acids solution (100×)] 10 mM Trypsin ethylenediamine tetra-acetic acid (1×) 0.05%/0.02% in DPBS (A&E Scientific), Dulbecco's Phosphate Buffered Saline (PBS) (Sigma-Aldrich), CellTiter-Glo® Luminescent Cell Viability Assay (Promega), Sephadex G75, and G100 (Sigma-Aldrich).

B. Preparation of the nanoparticles: PDA-PEG crosslinked copolymer nanoparticles

A PEG stock solution was prepared by dissolving PEG in 5 ml phosphate buffer (100 mM, *p*H 8.5) to give a 25 mM solution. The solution *p*H was adjusted to 8.5 with 1M HCl and 1M NaOH. Sufficient amounts of MilliQ water were added to give a final concentration of 23.4 mM, and this stock solution was stored at 4 °C. For the polymerization reaction, 225–900 μl of the PEG stock solution was added to the glass vial, and then phosphate buffer (100 mM, *p*H 8.5) was added to receive a final volume of 950 μl. Dopamine hydrochloride (10 mg, 52.7 μmol) was dissolved in 250 μl MilliQ water. 50 μl of the dopamine solution was added to the glass vial. The reaction mixture was mildly stirred overnight at room temperature, and the formed nanoparticles were purified by passing the solution through a Sephadex G-75 gel filtration column with MilliQ water and the first dark black-brown band was collected. This standard procedure was used for all further studies unless otherwise noted.

For the preparation of fluorescently labeled nanoparticles, fluorescein isothiocyanate (FITC) or rhodamine isothiocyanate (RITC) was dissolved in dimethyl sulfoxide at a final concentration of 1 mg/ml. The PDA-PEG crosslinked copolymer nanoparticles were suspended in phosphate buffer, *p*H 8.5, at a final concentration of 2 mg/ml. The FITC or RITC solution was added to the PDA-PEG nanoparticle solution at a mole ratio of 1:5 (fluorophore to amine: 76 nmol amines/mg nanoparticle), and the solution was incubated overnight under mild stirring. The formed nanoparticles were purified by passing the solution though a Sephadex G-75 gel filtration column with MilliQ water, and the first fluorescent band was collected [Fig. SI1 (Ref. 42)].

C. Particles characterization

1. NMR spectroscopy

To obtain information on the chemical environment of the samples, a set of NMR experiments was accomplished. ^{1}H NMR spectra of the solutions were recorded on a Bruker 850 MHz AVANCE III spectrometer in D_2O.

2. Dynamic light scattering

The PDA-PEG nanoparticles were diluted to a concentration of 100 μg/ml in MilliQ water and filtered through a 220 nm filter (Millipore, HA). Photon correlation spectroscopy was performed on an ALV5000 setup using a coherent solid state cw laser at $\lambda = 532$ nm with a power of 194 mW. The intensity autocorrelation function G(q,t) was recorded at different scattering wave vectors, $q = (4\pi n/\lambda)\sin(\theta/2)$ with n being the solvent refractive index was varied by changing the scattering angle θ between 15° and 150°, for water at 293 K, n = 1.333. The desired relaxation function, $C(q,t) = [G(q,t) - 1]^{1/2}$ analyzed by an inverse Laplace transformation

$$C(q, t) = \int_{-\infty}^{\infty} L(\ln \tau)\exp\left(\frac{-t}{\tau}\right) d\ln \tau \quad (1)$$

(CONTIN algorithm) yielding the distribution $L\ln(\tau)$ of relaxation times, τ. The most probable relaxation time for the contributing processes is obtained from the peak positions of $L\ln(\tau)$ and the corresponding intensity $I_i(q) = a_i(q)I(q)$ of the i-th process is computed from the total light scattering

intensity I(q) and the amplitude

$$a_i = \int L(\ln \tau) d \ln \tau \quad (2)$$

over the i-th peak in L ln(τ).

3. Cryo-TEM

Frozen vitrified samples were prepared by applying an aqueous solution of PDA-PEG nanoparticles on a lacey carbon TEM grid. Subsequently, excess solution was blotted off by a filter paper and the TEM grid was plunged in liquid ethane immediately (FEI Vitrobot). Cryo-TEM measurements were performed on a FEI Tecnai F20 at an acceleration voltage or 200 kV. Micrographs were taken with a CCD Camera (Gatan US1000) using low dose conditions in order to minimize beam damage.

4. Thermogravimetric analysis

Thermogravimetric analysis (TGA) was performed using a TGA/DSC 3+/HT/1600/274 (Mettler Toledo) under nitrogen applying a heating rate of 10 K/min.

5. Zeta potential

The zeta potential of the PDA-PEG nanoparticles was evaluated with Zetasizer Nano-Z, Nano Series, Malvern. The PDA-PEG nanoparticles were diluted with an aqueous 10^{-3}M KCl solution. These measurements were performed in triplicates.

6. Ninhydrin assay

0.8 g of ninhydrin was dissolved in absolute ethanol. PDA-PEG nanoparticles were diluted in 200 mM acetate buffer, *p*H 5.5 to a concentration of 2 mg/ml. 80 μl of PDA-PEG nanoparticle solution was added to an empty well of a 384-well transparent cell culture plate. 20 μl of ninhydrin solution was added and the solution pipetted up and down to mix. The absorbance at 570 nm was measured and recorded as a reference. The culture plate was placed in an incubator at 60 °C for 45 min with shaking. The absorbance at 570 nm was read and recorded as a reference. The same procedure was repeated with various concentrations of glycine to obtain a standard curve. This was used to determine the number of amines present on the PDA-PEG nanoparticles.

7. Time-of-flight secondary ion mass spectrometry

A dried-droplet deposition of the PDA-PEG nanoparticles prepared on Al-foil was analyzed by 30 keV Bi_3 primary ions (TOF.SIMS NCS, IONTOF, Münster, Germany) to elucidate the surface chemistry of the particles. Surface spectra were acquired at a mass range of 1–2000 Da by applying a primary ion dose of 1.25×10^8 ions on $200 \times 200\,\mu m^2$ well below the static limit. Dual beam depth profiles were acquired using additionally 2.5 keV Ar_{1000} cluster ions for sample erosion on a field of view of $400 \times 400\,\mu m^2$ with a dose of 6.5×10^{11} ions.

D. *In vitro* characterization

1. Cell culture

The human alveolar basal epithelial carcinoma cell line A549 was obtained from DSMZ (German Collection of Microorganisms and Cell Cultures, Braunschweig). Cells were cultured in high-glucose DMEM supplemented with 10% FBS, 100 U/ml penicillin, 0.1 mg/ml streptomycin, and 0.1 mM nonessential amino acids at 37 °C in a humidified 5% CO_2 incubator.

2. Stability of PDA-PEG nanoparticles in the cell medium

The stability of PDA-PEG nanoparticles in the cell medium was investigated by dynamic light scattering (DLS). 0.1 ml of 1 wt. % of PDA-PEG nanoparticles in water was mixed with 0.25 ml of cell medium. The particle sizes at 0 h at 37 °C and 12 h of incubation at 37 °C were recorded to evaluate their stability.

3. Cell viability/cytotoxicity

A549 cells were plated onto a white 96-well plate at a density of 6500 cells/well and incubated overnight for attachment. The medium was removed and replaced with various concentrations of PDA-PEG nanoparticles suspended in cell media and incubated for another 4 or 24 h. Cells incubated with only fresh media were used as blank control. After the incubation period, the CellTiter Glo cell viability assay kit was used to quantify the viability of the cell culture in each well, according to the manufacturer's manual.

4. Cellular uptake

A549 cells were plated onto a white 96-well plate at a density of 6500 cells/well and incubated overnight for attachment. The medium was removed and replaced with varying concentrations of fluorescently labeled PDA-PEG nanoparticles suspended in media that were then incubated for another 4 or 24 h. Cells incubated with only fresh media were used as blank control. After the incubation period, the PDA-PEG nanoparticle solution was removed and each well was washed three times with PBS solution. Then, 50 μl of lysis buffer was added to each well and incubation proceeded overnight at 4 °C. The fluorescence of the cells was measured on a Tecan M1000 plate reader.

5. Confocal laser scanning microscopy

A549 cells were plated in an ibidi® 8-well ibiTreat, μ-slide at a density of 30 000 cells per well in 300 μl cell medium. The cells were incubated overnight at 37 °C in 5% CO_2 to allow adhesion. The next day, 100 or 500 μg/ml of fluorescently labeled PDA-PEG nanoparticles suspended in media was added to the wells, respectively, and incubated for 4 or 24 h. Before imaging, cells were washed three times with PBS buffer and 300 μl of fresh media. Imaging was then performed using an LSM 710 laser scanning confocal microscope system (Zeiss, Germany) coupled to an XL-LSM

710 S incubator and equipped with a 63× oil immersion objective. The emission of rhodamine-labeled nanoparticles was recorded using a 488 nm Argon laser for excitation and a 531–648 nm filter, whereas for fluorescein-labeled nanoparticles, a 515–565 nm filter was used. All acquired images were processed with ZEN software developed by Carl Zeiss.

To study the cellular uptake mechanism of PDA-PEG nanoparticles, A549 cells were plated onto a Greiner Bio-One™ CELLview™ Cell Culture Slides 10-well plate at a density of 75 000 cells/ml in 100 μl cell medium. The cells were incubated overnight for attachment at 37 °C in 5% CO_2. The next day, the medium was removed and replaced by 100 μg/ml of fluorescently labeled PDA-PEG nanoparticles suspended in cell medium. The cells were incubated at 4 °C without additional CO_2 or 37 °C in 5% CO_2 for 2 h. Before adding the PDA-PEG nanoparticles, the cells were preincubated at 4 °C for 0.5 h. For imaging, the cells were washed one time with DPBS and 100 μ/ml of fresh media was added. Imaging was then performed using a Leica TCS SP5 scanning confocal microscope system coupled to a 63× water immersion objective. The emission of rhodamine-labeled nanoparticles was recorded using a 515 nm Argon laser for excitation and 560–660 nm filter for emission.

III. RESULTS AND DISCUSSION

A. Synthesis of ultrasmall PDA-PEG crosslinked nanoparticles

Dopamine polymerizes to PDA via a number of reactive intermediates such as dopamine quinone, leukodopaminechrome, dopaminechrome, or 5,6 dihydroxindole (Fig. 1).[33,34] It is known that some of these intermediates as well as the oligomeric and polymeric PDA species containing quinone or unsaturated indole rings can react with various amine-containing molecules via Michael addition reactions and Schiff base formation reactions.[35] In order to install PDA and its intermediates as biocompatible crosslinkers, different amine-terminated PEG polymers of varying chain lengths and amine end groups were screened and nanoparticle formation was analyzed [see Tables I and SI1 (Ref. 42)]. For biological applications, it is essential to fully avoid organic solvents during particle formation, synthesis, and workup. Therefore, only water-soluble polymers with proven biocompatibility have been selected. Dopamine and the respective amine-terminated PEG derivatives of Tables I and SI1 (Ref. 42) were mixed in phosphate buffer. One mole equivalent of the amine-containing derivatives was added to dopamine HCl (2 mg/ml) in phosphate buffer at *p*H 8.5, and the mixture was incubated overnight. The formed nanoparticles were analyzed by employing DLS (Zetasizer) at one wave vector $q = 0.0314\ nm^{-1}$ (scattering angle $\theta = 173°$), and the respective results are listed in Tables I and SII (Ref. 42).

Only PEG derivatives with two terminal amino groups and molecular weights above 2000 g/mol were able to form very small and narrowly distributed nanoparticles. The combination of low molecular weight PEG (MW 220) or longer PEG chains with only one terminal amine group was not sufficient to stabilize small particle sizes, and instead larger particles or particle aggregates and high standard deviations indicating polydisperse samples were observed.

In order to contribute to an improved understanding of the molecular structure of PDA in the formed nanoparticles, the catechol monomer was varied as well and apart from dopamine, 1,2-dihydroxybenzene (catechol), dihydroxybenzylamine (DHBA), and L-3,4-dihydroxyphenylalanine (L-DOPA) [Fig. SI2 (Ref. 42), Table I] were studied. The amino acid L-DOPA is a natural bioprecursor of several neurotransmitters and melanin, and its molecular structure is similar to dopamine so that it undergoes intramolecular cyclization and forms 3D networks. When the catechol derivatives were mixed with bis-amino terminated $PEG3000(NH_2)_2$, stable nanoparticles were only formed with L-DOPA and dopamine indicating that internal cyclization and polymerization of the catechol derivative is necessary for nanoparticle formation (Table I). From these results, we developed a schematic of PDA-PEG nanoparticle formation, which is depicted in Fig. 1. Based on the dimensions of the formed nanoparticles and the obtained standard deviations, PDA nanoparticles prepared from α,ω-bis amine $PEG3000(NH_2)_2$ were selected for all further analyses [Table I, entry 4: PDA-$PEG3000(NH_2)_2$] as they were very narrowly dispersed and prepared from inexpensive, nonchiral dopamine starting material. The formed PDA-PEG nanoparticles were purified by passing the solution though a Sephadex G-75 gel filtration column with MilliQ water, and the first dark black-brown band was collected. The synthesis has been successfully upscaled to a batch size of 1 g, and the PDA-PEG nanoparticles were stable for several weeks at RT.

B. Characterization of PDA-PEG crosslinked copolymer nanoparticles

In order to obtain more insights into the chemical structure of the obtained PDA-PEG nanoparticles, a number of characterization methods have been applied. The ^1H NMR spectra of the precursors and the nanoparticles were analyzed, and the copolymer nanoparticles show all main signals corresponding to PDA and PEG [Figs. 2 and SI3 (Ref. 42)]. A clear shift of the PEG C-1 protons from 2.79 to 3.13 ppm (Fig. 2) was observed indicating the nucleophilic addition of the proximal amine group to the aromatic dopamine system (1,4 Michael addition or Schiff base reaction), which confirms the successful copolymerization of the dopamine/PEG monomers (Fig. 1). The FT-IR spectrum of the PDA-PEG nanoparticles reveals the signals of PEG and some signals of PDA. Compared with the spectrum of $PEG3000(NH_2)_2$ (Fig. 2), a broad absorbance peak at $1615\ cm^{-1}$ occurred for the PDA-PEG nanoparticles, which was assigned to the stretching vibration of the aromatic ring. In addition, the broad signal at $3420\ cm^{-1}$ was attributed to the catechol –OH groups of dopamine/PDA indicating that dopamine/PDA was incorporated. As the monomer dopamine hydrochloride also contains OH groups, the FT-IR spectrum of dopamine hydrochloride was compared to the FT-IR spectrum of PDA and PDA-PEG

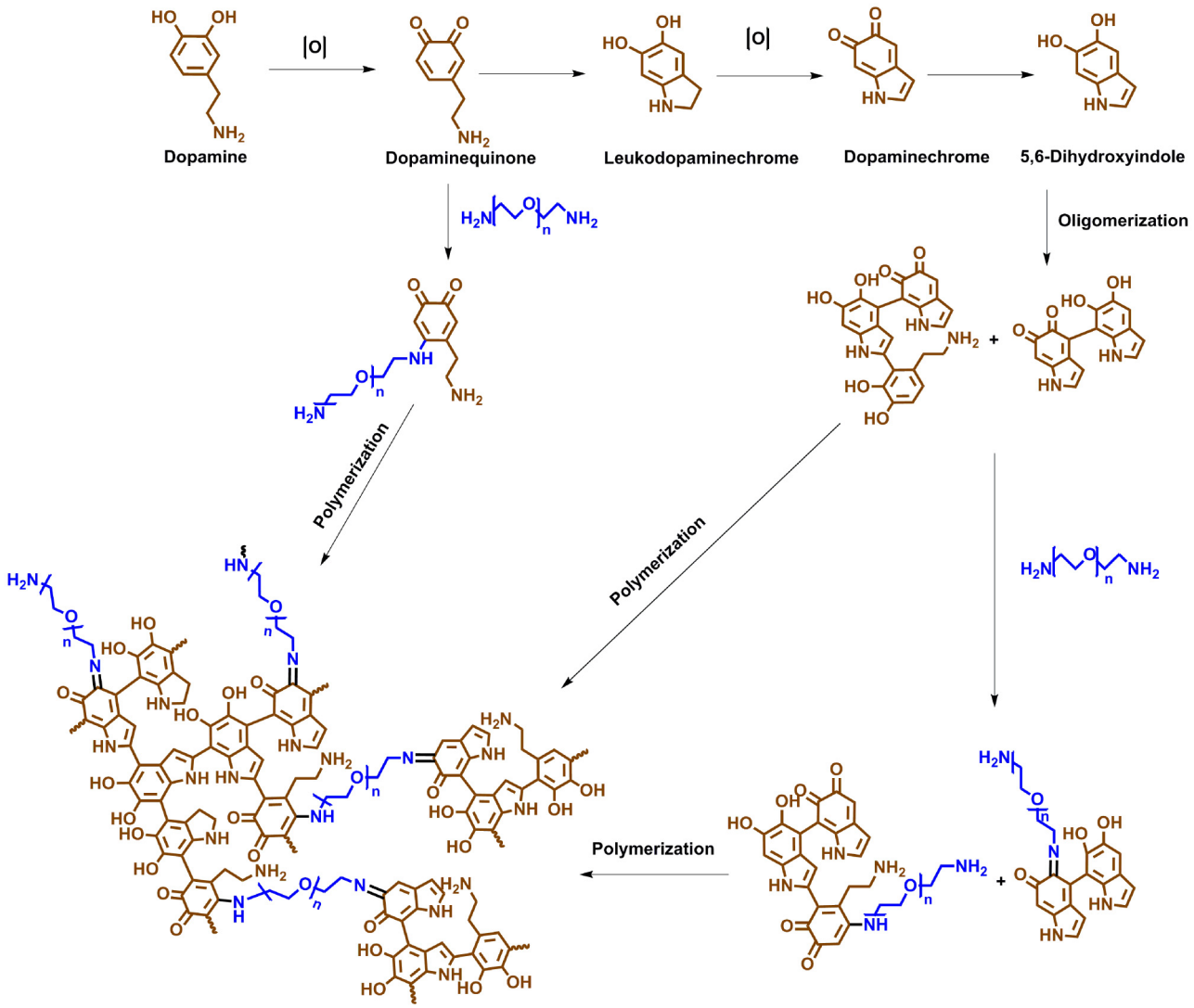

FIG. 1. Proposed schematic of PDA-PEG nanoparticle formation.

nanoparticles showing that there is a distinct difference between the nanoparticles and the PDA monomer in the fingerprint range (>1700 cm^{-1}) [Fig. SI4 (Ref. 42)] clearly supporting the formation of PDA species in the nanoparticles.

TABLE I. DLS results of nanoparticles formed with different amines (low/high molecular weight) or different catechol groups. Note that equimolar quantities were used for all experiments.

Expt. no.	Sample	Number mean (nm)	Stdev (nm)
1	Pure PDA	291	112.4
2	PDA-PEG220(NH_2)$_2$	275	144.8
3	PDA-PEG6000(NH_2)$_2$	41	4.3
4	PDA-PEG3000(NH_2)$_2$ "PDA-PEG"	18	0.65
5	PDA-PEG2000(NH_2)$_2$	22	2.7
6	PDA-PEG2000(NH_2)	99	7.8
7	Catechol-PEG3000(NH_2)$_2$	3.2	0.31
8	Poly(L-DOPA)-PEG3000(NH_2)$_2$	23	6.17
9	DHBA-PEG3000(NH_2)$_2$	2	0.51

The UV-vis spectra of the nanoparticle solutions, which appeared dark colored, showed the characteristic broadband absorbance of PDA. The TGA thermograms of PDA-PEG also supported copolymer formation as depicted in Fig. 2. A clear difference compared to pure PEG3000(NH_2)$_2$ was observed as the TGA thermogram for pure PDA showed a continuous weight loss of only 48% whereas sharp weight losses of 96% and 72% for the PEG and PDA-PEG nanoparticles, respectively, were observed at 400 °C indicating that PEG in the PDA-PEG nanoparticles decreases the thermal stability of PDA.

Interestingly, the compositional analysis of the PDA-PEG nanoparticles revealed approximately 60% of PEG and 40% of PDA (Fig. 2), which corresponds to approximately 13 dopamine molecules per 1 PEG chain.

Very high scattering vectors with q (q = 0.0314 nm^{-1}) were determined for all samples by DLS with the Zetasizer corresponding to the presence of only one particle population. However, due to the very high scattering vectors, slow populations corresponding to minor contributions of particles'

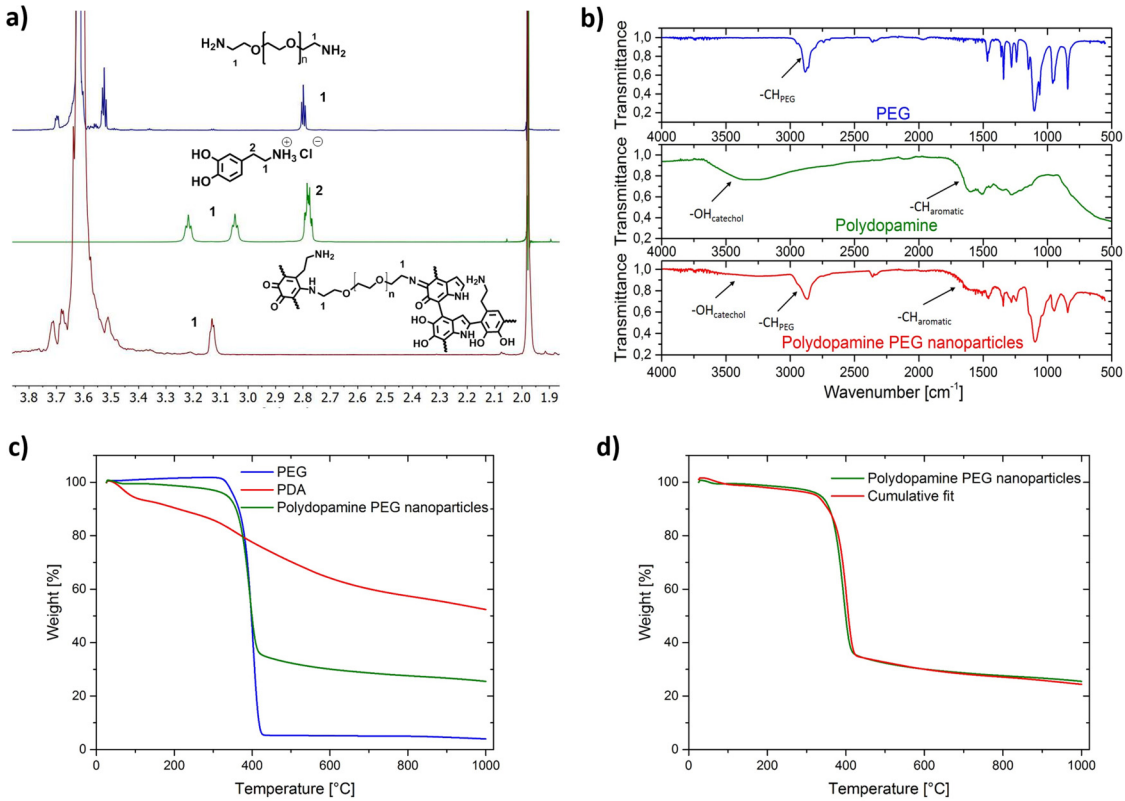

FIG. 2. (a) Assignment of the signals in the ^{1}H NMR spectrum of the PDA-PEG nanoparticles. Aliphatic region. *Top*: PEG3000. *Middle*: dopamine hydrochloride. *Bottom*: Nanoparticle reaction mixture (PDA-PEG). (b) FT-IR spectra of PEG3000$(NH_2)_2$ (top), PDA (middle), and of PDA-PEG. (c) TGA analysis. Individual thermograms. (d) Cumulative fit of data with 58.5 wt. % of PEG.

aggregates might be missed. Therefore, PDA-PEG was also analyzed in more sophisticated DLS experiments to uncover the dynamics and form factor over a broad q-range (note that q^{-1}'s represent the probing length scales). Figure 3(a) displays representative relaxation functions, C(q,t), and the corresponding exponential fits at two wave vectors, $q = 0.0157\,nm^{-1}$ (scattering angle $\theta = 60°$) and $0.0296\,nm^{-1}$ ($\theta = 140°$).

The inverse Laplace transformation analysis of the correlation function, C(q,t), now reveals the presence of two species as indicated by the bimodal shape of distribution function, Lln(τ) [black and red lines in the main plot in Fig. 3(a)]. The variation of D_i (upper inset) and the component intensities $I_i(q)$ (lower inset) are shown in the insets of Fig. 3(a). The analysis of the DLS plots of PDA-PEG nanoparticles in

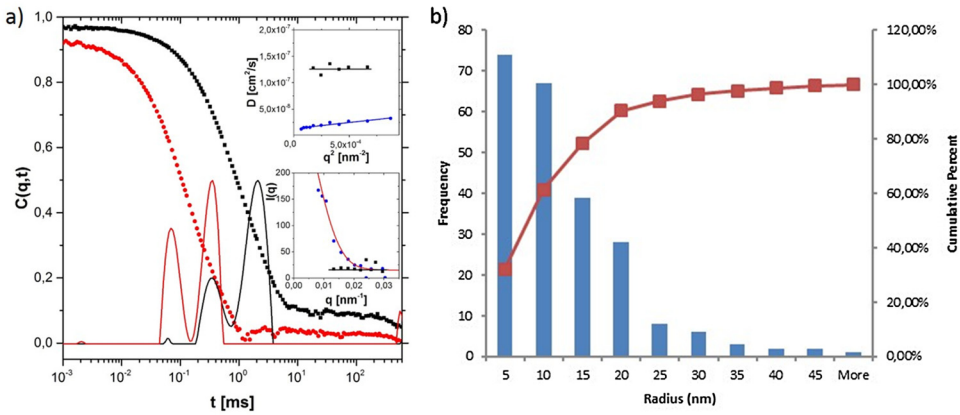

FIG. 3. (a) Relaxation function, C(q,t), of the PDA-PEG nanoparticles (100 μg/ml) at two wave vectors, $q = 0.0157\,nm^{-1}$ (black square) and $q = 0.0296\,nm^{-1}$ (red circle). Upper inset: The fast center of mass translation diffusion, D, of small size population (black square) independent of q yields an average radius of around 21 nm. The slow diffusion coefficient of large radius population (blue circle) increases with q^2 due to internal dynamics (Ref. 36). Low inset: The scattering intensity, I(q), associated with the large size (blue circle) dominates total intensity (solid line) at low angles and small size (black square) population. (c) Data histogram of the size distribution of PDA-PEG nanoparticles determined by cryo-TEM. The blue bars are the frequency and the red line is the cumulative percentage.

aqueous solution at different angles now revealed one major population of very small nanoparticles with a hydrodynamic radius $R_{h,f}$ of 21 ± 2 nm and about 2.5% of a second, minor population with a hydrodynamic radius $R_{h,s}$ of 186 nm [Fig. 3(a)]. Further details are described in the supporting information.[42] Cryo-TEM images of the nanoparticles support this conclusion with a mean radius of 18 ± 5 nm and some larger particles [Figs. 3(b) and SI5 (Ref. 42)].

To receive further information about the stability of the PDA-PEG nanoparticles, the zeta potential was measured at *p*H 7. The PDA-PEG nanoparticles have a negative zeta potential ($\zeta = -7.4 \pm 12.3$ mV), which is similar to, e.g., PEG-PLGA nanoparticles.[37] The PDA-PEG nanoparticles were further analyzed to determine if the available amines originated from the PDA from uncrosslinked PEG chains. The number of primary amine groups was quantified in a ninhydrin assay, where ninhydrin reacts with primary amines forming a purple dye with maximum absorbance at 570 nm. Using glycine, a standard curve was made and compared to the values obtained for PDA-PEG nanoparticles. About 76 nmol amines/mg of PDA-PEG nanoparticles were determined, which is a very small amount ($\ll 1\%$) considering that 3 mmol reactive amino groups (assuming that no amine groups had reacted) are present in 1 mg PEG-PDA nanoparticle [see supporting information (Ref. 42) for the calculations]. These results suggest that most of the amino groups of PEG have reacted and formed interconnecting loop crosslinked structures. The amino groups of PDA either remained inside of the nanoparticle and were nonaccessible for further reactions or they have formed five membered rings.

Based on these results, the supramolecular structures of the PDA-PEG nanoparticles consist of either (a) a dense PDA core and a PEG shell (PEG chains on the surface of the nanoparticles with extended chains or loops due to the usage of bis-amine PEG) or (b) the PEG chains could aggregate into spherical nanoparticles that are crosslinked by several smaller oligomeric or polymeric PDA nanostructures (brown) distributed within the PEG nanoparticle volume (Fig. 4). Previously, PEG nanoparticles have been obtained after acetylation or acrylation of one end of the PEG chain,[28] whereas oligocarbonatefluorene termini at both ends of the PEG chain formed self-assembled starlike micelles where the fluorene groups localized both inside the PEG micelle and in the shell (example in Fig. 4).[29]

Based on the obtained data, the internal structure of the PDA-PEG nanoparticles (diameter: 42 nm) cannot be entirely ruled out. However, considering that the nanoparticles consist of PDA-PEG with around 60 wt. % PEG and around 40 wt. % PDA, indicating about 13 dopamine molecules per 1 PEG chain, we can assume that the aromatic rings in PDA cluster into highly crosslinked oligomers that form hydrophobic domains within the PDA-PEG volume that are protected from water by the PEG shell. Time-of-flight secondary ion mass spectrometry (TOF-SIMS) surface analyses of the PDA-PEG nanoparticles confirm this assumption. The presence of secondary ion signals from both, PEG and PDA, on the topmost surface of the deposited PDA-PEG particles have been detected suggesting that both components are present at the surface of the particle as depicted in Fig. 4 [compare Table SI2 (Ref. 42)]. Furthermore, depth profiling analyses with Ar cluster sputtering show similar traces for both components indicating a constant ratio of PEG and PDA throughout the sputter erosion process as expected from Fig. 4 [Fig. SI6 (Ref. 42)]. Furthermore, it has been reported previously that in PDA films, dopamine oligomers first form nanoaggregates, which assemble into random aggregates on the micrometer scale.[38] Thus, it is likely that several PDA nanoaggregates are formed that crosslinked the more hydrophilic PEG chains producing a PEG network with inner PDA oligomeric or polymeric aggregates that are prevented from aggregation (Fig. 4).[39]

C. Functionalization of the PDA-PEG nanoparticles

Postmodification of the nanoparticles is necessary to impart higher functional diversity, i.e., to attach guest molecules or to control transport into cells. Importantly, the structure of the nanoparticles should not be adversely altered after modification. According to the proposed PDA-PEG growth mechanism, free primary amino groups should be present in

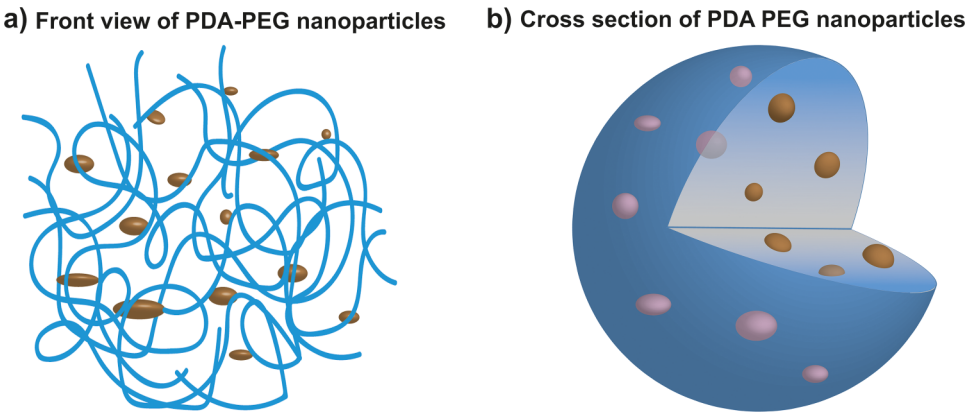

FIG. 4. Schematic illustration of the PDA-PEG copolymer nanoparticles based on the experimental results. PDA molecules (brown) are distributed all over the PEG (blue) nanoparticle. (a) Front view; (b) Cross section.

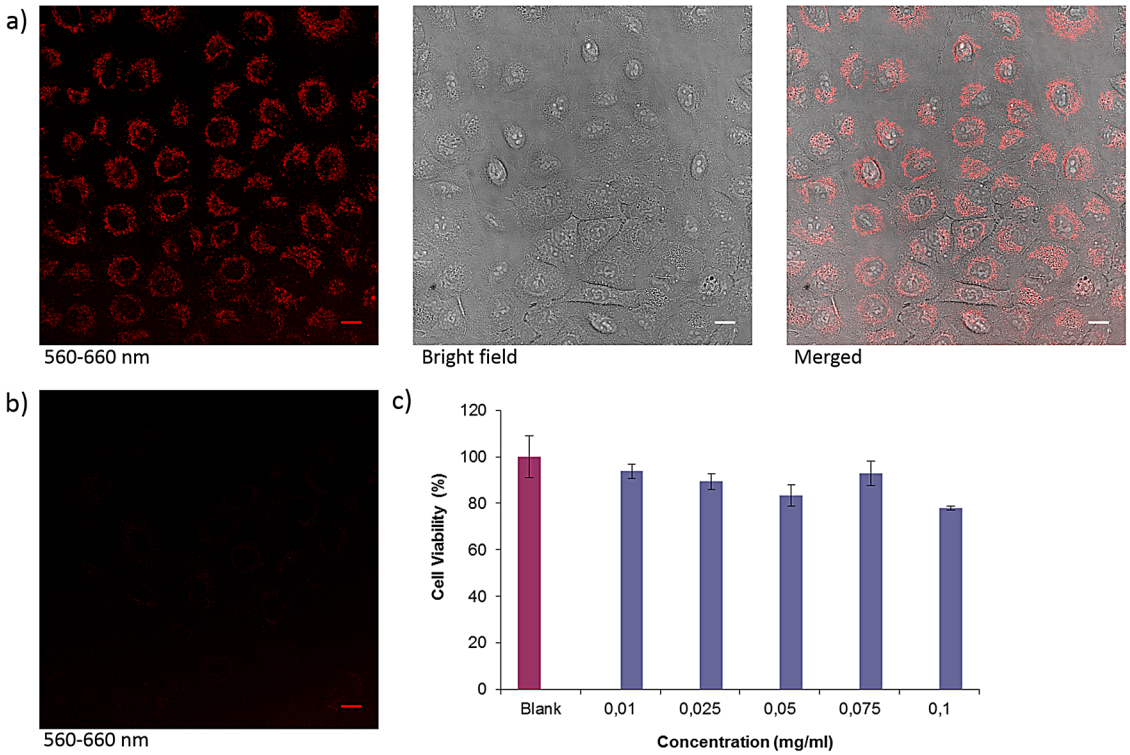

FIG. 5. Confocal images of rhodamine-labeled PDA-PEG nanoparticles (100 μg/ml) in A549 cells, 2 h incubation at 37 °C (a), at 4 °C (b). Scale bars in (a) and (b): 20 μm. The images of the blank cells are shown in the supporting information (Fig. SI8) (Ref. 42). Cell viability after treatment with PDA-PEG nanoparticles at the concentration of 0–0.1 mg/ml (c).

the nanoparticles, which is essential for further functionalizations. FITC or RITC, amine reactive fluorescent dyes, was mixed with the PDA-PEG nanoparticles in phosphate buffer, *p*H 8.5, and left to react overnight. During purification by size exclusion chromatography, two fluorescent bands were detected. The band corresponding to the faster moving species was assigned to the successfully dye-labeled PDA-PEG nanoparticles, whereas the slower moving species was assigned to the free dye. In this way, the dye-labeled PDA-PEG nanoparticles could be purified and the free dye was removed [Fig. SI4 (Ref. 42)].

D. Cytotoxicity and cell uptake of PDA-PEG crosslinked copolymer nanoparticles

Due to the small sizes, the opportunities to impart functionalities, and the application of nontoxic monomers such as PEG and dopamine as well as no detergents and organic solvents, the PDA-PEG nanoparticles provide many attractive features as biomaterial and nanocarrier system. First, DLS studies were performed to prove that the PDA-PEG nanoparticles remained stable in cell medium [Fig. SI7 (Ref. 42)]. Then, PDA-PEG nanoparticles labeled with isothiocyanate fluorescent dyes (FITC or RITC) were added to the cultured A549 lung carcinoma epithelial cells and cellular uptake and cytotoxicity were investigated.

Confocal laser scanning microscopy revealed an efficient and homogenous uptake at 100 μg/ml. Moreover, the internalization process was surprisingly rapid (4 h) given the high PEG content in the nanoparticles. In contrast, PEGylated species such as PEGylated dyes, nanoparticles, or micelles and PEG functionalized dyes (perylenedicarboxmonoimide, benzoylterrylen-3,4-dicarboximide[40] functionalized with one PEG chain or dendritic polyglycerol perylene imido dialkylester)[41] are known to penetrate mainly into the outer cell membrane (as demonstrated by membrane labeling experiments) and they did not reveal significant cellular uptake as demonstrated for PDA-PEG. To shed further light on the cellular uptake mechanism of PDA-PEG nanoparticles, cellular uptake experiments were performed at 4 °C to minimize the contribution of active cellular processes. The results were compared to the experiments performed at 37 °C [Figs. 5(a) and 5(b)]. Obviously, PDA-PEG nanoparticles entered the cells via energy dependent receptor-mediated cell uptake [Fig. SI8 (Ref. 42)] since no internalization of nanoparticles was observed at 4 °C. Cytotoxicity studies analyzed by Cell-TiterGlo gave an IC_{50} value of about 500 μg/ml indicating high cell compatibility [Fig. 5(c)].

IV. SUMMARY AND CONCLUSIONS

In summary, PDA-PEG nanoparticles of less than 50 nm in diameter have been prepared in a simple one-step reaction soley in aqueous solution, which has been a challenge in the past. The polymerization of dopamine and $PEG(NH_2)_2$ proceeds rapidly in aqueous solution (phosphate buffer) at room temperature, which is efficient, scalable, and convenient. The particles had defined sizes in the range of 40 nm, and no

sedimentation was detected most likely due to the formation of an outer protecting PEG shell. The exact inner structure of the nanoparticles cannot be ruled out entirely and the formation of a dense PDA core or several PDA nanoaggregates are likely. The PDA-PEG nanoparticles provide high water solubility and high colloidal stability in buffer, and the availability of accessible free amino groups has been clearly demonstrated. PDA-PEG crosslinked copolymer nanoparticles reveal improved colloidal and biological stabilities compared to PDA nanoparticles, which makes them very attractive for biomedical applications. High cell viability suggests that the PDA-PEG nanoparticles could be biocompatible and more importantly, their cellular uptake and internalization process proceeded rapidly opening various opportunities for drug delivery and cellular bioimaging. This novel route for facile and convenient PDA-PEG copolymer fabrication solely in aqueous solution provides great potential for future biomedical applications. Further studies to clarify the internal structure and the exact mechanism of PDA-PEG nanoparticles are currently ongoing.

ACKNOWLEDGMENTS

The authors acknowledge support by the BMBF (Biotechnologie 2020 + initiative, "Selekomm" project) and the European Research Council (ERC, Synergy Grant No. 319130-BioQ and ERC, Advanced Grant No. 694977-SmartPhon) and Open Access funding provided by the Max Planck Society. This work is supported by the Collaborative Research Center (CRC) Transregio 234, which is supported by the German Research Foundation. The authors thank Manfred Wagner for the NMR measurements, Eva Deister for the TGA measurements of the crosslinked polydopamine PEG copolymer nanoparticles, Werner Steffen for technical support during the light scattering measurements, Antje Larsen for help with the fit of the light scattering results, Christine Rosenauer for DLS measurements of PDA-PEG nanoparticles in cell medium, and Tommaso Marchesi D'Alvise for support with drawing of the figures.

[1]K. M. El-Say and H. S. El-Sawy, Int. J. Pharm. **528**, 675 (2017).
[2]L. Wang, P. Zhao, C. Feng, Y. Wu, Y. Ding, and A. Hu, Eur. Polym. J. **105**, 1 (2018).
[3]C. Wu and D. T. Chiu, Angew. Chem. Int. Ed. **52**, 3086 (2013).
[4]J. Yang, S. Zhai, H. Qin, H. Yan, D. Xiang, and X. Hu, Biomaterials **176**, 1 (2018).
[5]M. Elsabahy and K. L. Wooley, Chem. Soc. Rev. **41**, 2545 (2012).
[6]Y. Wu, S. Ihme, M. Feuring-Buske, S. L. Kuan, K. Eisele, M. Lamla, Y. Wang, C. Buske, and T. Weil, Adv. Healthcare Mater. **2**, 884 (2013).
[7]S. K. Nitta and K. Numata, Int. J. Mol. Sci. **14**, 1629 (2013).
[8]V. Ball, Catal. Today **301**, 196 (2018).
[9]X. Wang, J. Zhang, Y. Wang, C. Wang, J. Xiao, Q. Zhang, and Y. Cheng, Biomaterials **81**, 114 (2016).
[10]D. Zhang, M. Wu, Y. Zeng, L. Wu, Q. Wang, X. Han, X. Liu, and J. Liu, ACS Appl. Mater. Interfaces **7**, 8176 (2015).
[11]S. Sieste *et al.*, Adv. Healthcare Mater. **7**, 1701485 (2018).
[12]Z.-H. Miao, H. Wang, H. Yang, Z.-L. Li, L. Zhen, and C.-Y. Xu, ACS Appl. Mater Interfaces **7**, 16946 (2015).
[13]K.-Y. Ju, Y. Lee, S. Lee, S. B. Park, and J.-K. Lee, Biomacromolecules **12**, 625 (2011).
[14]C.-C. Ho and S.-J. Ding, J. Mater. Sci. Mater. Med. **24**, 2381 (2013).
[15]X. Jiang, Y. Wang, and M. Li, Sci. Rep. **4**, 6070 (2015).
[16]F. Ponzio, P. Bertani, and V. Ball, J. Colloid Interface Sci. **431**, 176 (2014).
[17]N. F. Della Vecchia, A. Lichini, A. Napolitano, G. D'Errico, G. Vitiello, N. Szekely, M. d'Ischia, and L. Paduano, Langmuir **30**, 9811 (2014).
[18]X. Zhang, S. Wang, L. Xu, L. Feng, Y. Ji, L. Tao, S. Li, and Y. Wei, Nanoscale **4**, 5581 (2012).
[19]Z. Wang *et al.*, Part. Part. Syst. Char. **33**, 89 (2016).
[20]X. Yu, H. Fan H, L. Wang, and Z. Jin, Angew. Chem. Int. Ed. **53**, 12600 (2014).
[21]J. Cui, Y. Yan, G. K. Such, K. Liang, C. J. Ochs, A. Postma, and F. Caruso, Biomacromolecules **13**, 2225 (2012).
[22]F. Branda, B. Silvestri, G. Luciani, A. Costantini, and F. Tescione, Colloids Surf. A Physicochem. Eng. Aspects **367**, 12 (2010).
[23]F. Liu, X. He, J. Zhang, H. Chen, H. Zhang, and Z. Wang, J. Mater. Chem. B Mater. Biol. Med. **3**, 6731 (2015).
[24]A. Chassepot and V. Ball, J. Colloid Interface Sci. **414**, 97 (2014).
[25]C. Bergtold *et al.*, Biomacromolecules **19**, 3693 (2018).
[26]X. Zhong, K. Yang, Z. Dong, X. Yi, Y. Wang, C. Ge, Y. Zhao, and Z. Liu, Adv. Funct. Mater. **25**, 7327 (2015).
[27]J. Park, T. F. Brust, H. J. Lee, S. C. Lee, V. J. Watts, and Y. Yeo, ACS Nano **8**, 3347 (2014).
[28]J. Pang, F. Wu, C. Liao, Z. Gu, and S. Zhang, Biomacromolecules **18**, 1956 (2017).
[29]V. M. Prabhu, S. Venkataraman, Y. Y. Yang, and J. L. Hedrick, ACS Macro Lett. **4**, 1128 (2015).
[30]Z. Ma and X. J. Zhu, Mol. Pharm. **15**, 2348 (2018).
[31]H. Y. Yang, M.-S. Jang, G. H. Gao, J. H. Lee, and D. S. Lee, Nanoscale **8**, 12588 (2016).
[32]S. A. A. Kooijmans, L. A. L. Fliervoet, R. van der Meel, M. H. A. M. Fens, H. F. G. Heijnen, P. M. P. van Bergen en Henegouwen, P. Vader, and R. M. Schiffelers, J. Control. Release **224**, 77 (2016).
[33]H. Lee, S. M. Dellatore, W. M. Miller, and P. B. Messersmith, Science **318**, 426 (2007).
[34]S. Hong, Y. S. Na, S. Choi, I. T. Song, W. Y. Kim, and H. Lee, Adv. Funct. Mater. **22**, 4711 (2012).
[35]J. Yang, M. A. C. Stuart, and M. Kamperman, Chem. Soc. Rev. **43**, 8271 (2014).
[36]K. Wunderlich, A. Larsen, J. Marakis, G. Fytas, M. Klapper, and K. Müllen, Small **10**, 1914 (2014).
[37]Y. A. Haggag, K. B. Matchett, H. Dakir El, P. Buchanan, M. A. Osman, S. A. Elgizawy, M. El-Tanani, A. M. Faheem, and P. A. McCarron, Int. J. Pharm. **521**, 40 (2017).
[38]D. J. Miller, D. R. Dreyer, C. W. Bielawski, D. R. Paul, and B. D. Freeman, Angew. Chem. Int. Ed. **56**, 4662 (2017).
[39]J.-H. Jiang, L.-P. Zhu, L.-J. Zhu, B.-K. Zhu, and Y.-Y. Xu, Langmuir **27**, 14180 (2011).
[40]T. Weil, M. A. Abdallah, C. Jatzke, J. Hengstler, and K. Müllen, Biomacromolecules **6**, 68 (2005).
[41]T. Heek, J. Nikolaus, R. Schwarzer, C. Fasting, P. Welker, K. Licha, A. Herrmann, and R. Haag, Bioconjug. Chem. **24**, 153 (2013).
[42]See supplementary material at https://doi.org/10.1116/1.5042640 for further information about the characterization of PDA-PEG nanoparticles.

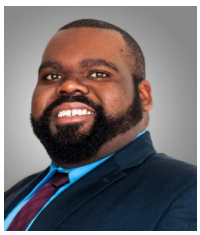

Sean Harvey received Bachelor degrees in Biochemistry and Chemical Engineering from Virginia Tech in 2007. After 5 years of working as an engineer for the US Department of Defense, he began studies in Biomaterials at Ulm University in Germany where he graduated with a Master of Science in December 2017. Sean completed his master thesis in the group of Prof. Dr. Tanja Weil. He continued his research with Prof. Dr. Tanja Weil, moving with her to the Max Planck Institute for Polymer Research. Here, he

is exploring polydopamine as a versatile building block as part of his Ph.D. research.

David Yuen Wah Ng studied chemistry at the National University of Singapore and received his B.Sc. with first class honours in 2009. In 2010, he received a scholarship at Max Planck Institute for Polymer Research and moved with Prof. Dr. Tanja Weil to Ulm to work on synthesizing bioactive dendrimer-protein conjugates David received his doctorate with *summa cum laude* in 2014 and worked as a group leader in the Institute of Organic Chemistry III at Ulm University until 2016. Since 2016, he leads the synthetic lifelike nanosystems group in the Department of Synthesis of Macromolecules at the Max Planck Institute for Polymer Research.

Jolanta Szelwicka studied Chemistry at the University of Wroclaw in Poland where she got her Bachelor of Science degree in 2010. After parental leave she continued Chemistry at the Johannes Gutenberg University Mainz. She joined the group of Prof. Dr. Tanja Weil for her master thesis in September 2017 at the Max Planck Institute for Polymer Research in Mainz where she worked on the synthesis and characterization of polydopamine thin films.

Lisa Hueske studies biomedicine chemistry at the Johannes Gutenberg University in Mainz and graduated with a Bachelor of Science in March 2016. She continued with her master study in biomedicine chemistry and moved to the Max Planck Institute for Polymer Research for her master thesis, where she works on polydopamine nanoparticle and films for biological applications.

Lothar Veith received his B.Sc. and M. Sc. degrees in chemistry from the University of Goettingen in 2010 and from the University of Muenster in 2012. He pursued his Ph.D. at the surface-analytical laboratory Tascon GmbH exploring the detection of nanoparticles in tissue sections by Time-of-Flight Secondary Ion Mass Spectrometry. In 2018, Lothar joined the group of Prof. Dr. Tanja Weil team at the Max Planck Institute for Polymer Research, where he is now part of the mass spectrometry research group focusing on mass spectrometric imaging, combinations with complementary techniques and Time-of-Flight Secondary Ion Mass Spectrometry.

Marco Raabe studied at Ulm University (Germany) where he received his bachelor degree in biochemistry in 2013. Afterwards, he continued at Ulm University for his master degrees in biochemistry. In 2015, he performed his master thesis in the group of Tanja Weil and focused on protein modification inspired by nature. He stayed in the group of Tanja Weil for his Ph.D. and moved with her to the MPIP in July 2016. His research focus is on biopolymeric coating of nanodiamonds for targeted delivery and biomedical imaging. His work is part of the EU-Project Hyperdiamond (Horizon 2020).

Ingo Lieberwirth is the head of the electron microscopy core facility of the Max Planck Institute for Polymer Research. His work focuses on the crystallization of precision polymers, on the formation and visualization of the protein corona on nanoparticles, and on correlative microscopy for the identification of intracellular nanoparticles.

George Fytas is professor of Physical Chemistry in the Department of Materials Science & Technology of the University of Crete, affiliated member of IESL/FORTH and External Member of the Max Planck Institute for Polymer Research in Mainz. George Fytas has received the B.S. in Chemistry Department of the University of Athens and the Ph.D. from the Technical University of Hannover in Germany. He performed his postdoc research in SUNY at Stony Brook in USA and received his habilitation from the University of Bielefeld in Germany. Among other numerous awards, he received a Humboldt Senior Research Award (2002), became a Fellow of the American Physical Society (2004) and he received an ERC Advanced Grant (2015).
His mission is the basic understanding and prediction of the behavior and tunability of unconventional physical properties of structured soft materials with spatiotemporal complexity.

Katrin Wunderlich obtained a joint degree in chemistry and chemical engineering from both the University of Würzburg and Ecole Supérieure de Chimie Physique Electronique de Lyon in 2009. During her subsequent Ph.D. under the guidance of Prof. Dr. K. Müllen at the Max Planck Institute for Polymer Research (MPIP) in Mainz, she developed amphiphilic hexaphenylbenzene and hexa-peri-hexabenzocoronene derivatives and studied their self-assembly, during which she was awarded a competitive Ph.D. fellowship of the German Association of the Chemical Industry. In 2014, she worked as a postdoc at the Weizmann Institute of Science, Rehovot,

Israel in the group of Prof. Jacob Klein, funded by a Dean of Faculty Fellowship of the Weizmann Institute of Science. In September 2014, she became a project leader at the MPIP in the department of Prof. Dr. K. Müllen. Since 2017, she has a project leader position in the group of Prof. Dr. Tanja Weil. She develops polydopamine particles and ultrathin functional hybrid films. Additionally, her research goal is to gain deeper insights how molecules self-assemble and how this process affects the resulting properties of the formed materials.

Tanja Weil studied chemistry (1993–1998) at the TU Braunschweig (Germany) and the University of Bordeaux I (France) and completed her Ph.D. at the MPI for Polymer Research with Klaus Müllen. From 2002 to 2008, she managed different leading positions at Merz Pharmaceuticals GmbH (Frankfurt) from Section Head Medicinal Chemistry to Director of Chemical Research and Development. She accepted an Associate Professor position at the National University of Singapore in 2008. In 2010, she joined Ulm University as Director of the Institute of Organic Chemistry III/Macromolecular Chemistry. Tanja Weil became member of the Max Planck Society in 2017 as one of the directors of the Max Planck Institute for Polymer Research heading the department "Synthesis of Macromolecules." She has received the Otto Hahn Medal of the Max Planck Society (2003), an ERC Synergy Grant together with Fedor Jelezko and Martin Plenio (2013) and the research prize of the city of Ulm (2014). Her current scientific interests include the synthesis of quantum materials, functional macromolecular architectures, and biohybrid materials to address urgent challenges in materials science, biomedicine, and sensing.